Journal of Structural Geology, Vol. 12, No. 7, pp. 823 to 833, 1990
Printed in Great Britain

0191-8141/90 $03.00+0.00

Quartz fabric evolution within the Adra Nappe (Betic Cordilleras, Spain)

JULIA CUEVAS and JOSÉ M. TUBÍA

Departamento de Estratigrafía, Geodinámica y Paleontología. Facultad de Ciencias, Universidad del País Vasco, 48080 Bilbao, Spain

(*Received* 24 *July* 1989; *accepted in revised form* 22 *February* 1990)

Abstract—The Adra Nappe (Alpujárride Complex, Betic Cordilleras) is an imbricated thrust sheet of metamorphic rocks. At the regional scale, changes in *c*-axis fabrics of deformed quartzites in the nappe are fully consistent with the strain path inferred from the microstructures. In the upper part of each imbricate, where the reference frame (S_2, L_2) is weakly deformed by open F_3-folds, quartz *c*-axis fabrics are characterized by symmetrical patterns of small-circle girdles around Z. Increasing strain towards the basal thrust faults is marked by new quartz fabrics developed during a pervasive D_3-mylonitization. These fabrics correspond to asymmetrical single-girdles or asymmetrical type II cross-girdles.

These changes in quartz fabric can be correlated with the progressive replacement of an initial coaxial flow (D_2) by a non-coaxial flow (D_3) near the thrust fault, as a result of the movement of the Adra Nappe.

INTRODUCTION

FABRIC studies during the last decade has shown that quartz microstructures and *c*-axis fabrics are powerful tools in unraveling the kinematics of plastically deformed tectonites in ductile shear zones. This is largely based on the close relationship between the type of symmetry of crystallographic fabrics and the flow regime, as inferred from theoretical approaches to the development of preferred crystallographic orientations (Etchecopar 1974, 1977, Lister 1981) and from fabric analyses of natural tectonites (Bouchez 1977, Burg & Laurent 1978, Bouchez & Pêcher 1981, Behrmann & Platt 1982, Simpson & Schmid 1983). In addition, experimental deformation of quartz analogs such as ice (Bouchez & Duval 1982, Burg *et al.* 1986) and experimental deformation of quartz itself (Tullis *et al.* 1973, Kirby 1977) supports these kinematic interpretations. From these studies it follows that petrofabric analysis can serve to establish strain-partitioning within a geological structure, both at the outcrop (Carreras *et al.* 1977, García-Celma 1982) and at a regional scale (Lister & Dornsiepen 1982, Law *et al.* 1984).

This paper investigates quartz *c*-axis fabrics within a thrust sheet in the Betic Zone of southern Spain, with particular reference to the following aspects: (1) the way in which the quartz fabric was modified as a consequence of the history of progressive deformation undergone by the nappe; (2) the possibility that symmetrical *c*-axis fabrics within mylonite zones in some cases reflect the fabric-memory of the pre-mylonitic deformation; and (3) the lithological control on fabric evolution in rocks with different quartz content, during a progressive deformation and, consequently, the influence of the lithology on the mechanisms which favour the acquisition of plastic deformation in tectonites.

With these aims in mind we present a petrofabric analysis of the Adra Nappe, which belongs to the Alpujárride Complex of the Betic Cordilleras in Southern Spain. This study builds on previous structural studies of the nappe (Aldaya 1969, Cuevas 1988), which have constrained its deformation history and metamorphic evolution as well as its movement direction.

GEOLOGICAL SETTING

In the Betic Cordilleras two major domains can be distinguished (Fig. 1a). (1) The External Zones to the north are related to the South-Iberian palaeomargin. These are formed mainly by sedimentary rocks of Mesozoic and Tertiary ages. (2) The Betic Zone to the south, consists mainly of metamorphic materials of Triassic age or older (Egeler & Simon 1969). On the basis of their lithological and metamorphic characteristics and their structural position the Betic Zone is divided into three main complexes (Julivert *et al.* 1973): the lowermost Nevado-Filábride Complex; the intermediate Alpujárride Complex and the uppermost Maláguide Complex.

The Adra Nappe, the subject of the present study, belongs to the Alpujárride Complex. The Alpujárride Complex is composed by several nappes which present a metapelitic sequence affected by a low to intermediate *P–T* metamorphism. The metamorphism decreases towards the top in each nappe, while on a regional scale, the highest grade nappes occur at the highest structural levels (Aldaya *et al.* 1979).

The Adra Nappe

The Adra Nappe is an imbricated thrust sheet which consists of a sequence with migmatites at the base, overlain by a sequence of schists with a decreasing metamorphism upwards (with sillimanite, staurolite, garnet and biotite). The schists are overlain by phyllites of Permian–Triassic ages and by a formation of Triassic marbles. This nappe has been displaced from the SW to the NE, along ductile mylonite zones. A later movement

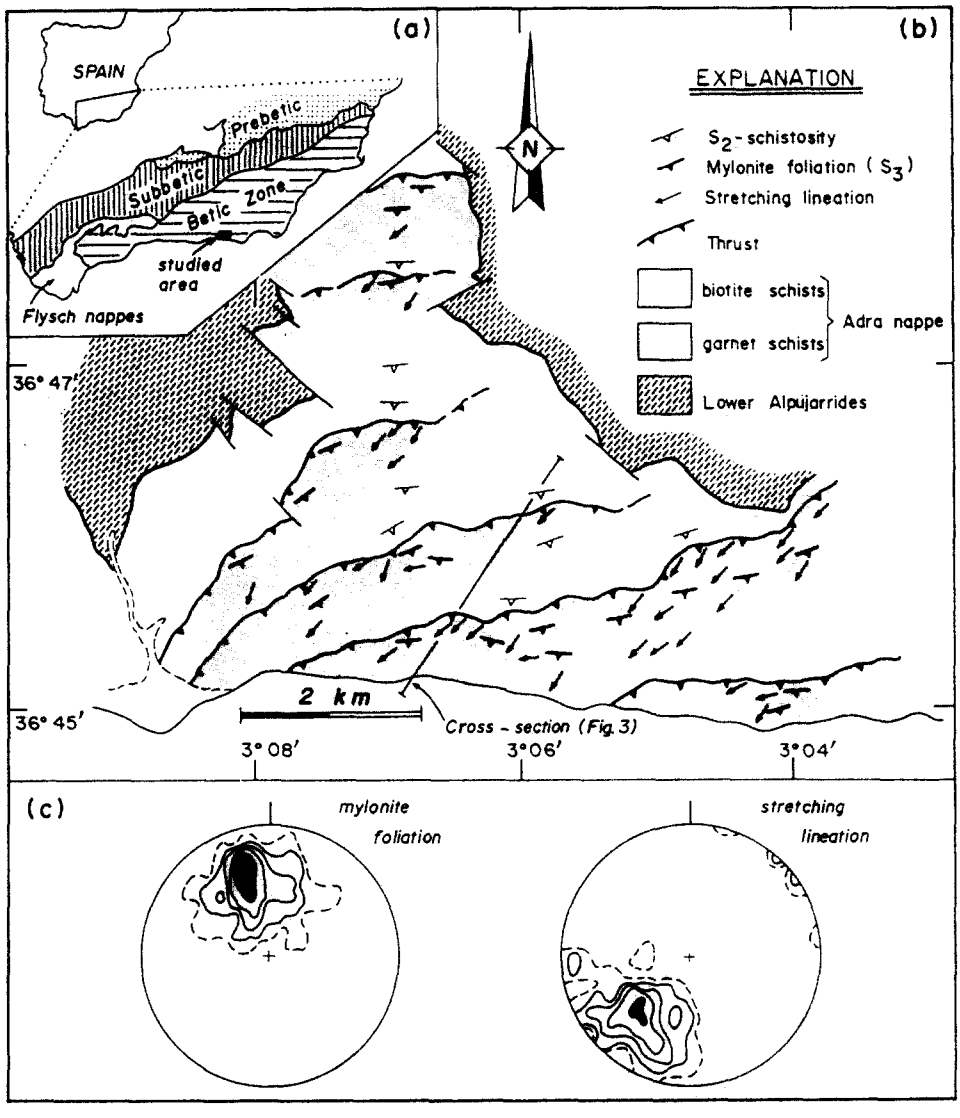

Fig. 1. (a) Tectonic sketch map of the Betic Cordilleras, showing the setting of the Adra sector within the Betic Zone. (b) Simplified geological map of the central part of the Adra Nappe. (c) Lower-hemisphere, equal-area projections of mylonite foliations (420 measurements; contours: 1, 3, 7, 10 and ≥15% per 1% area) and stretching lineations (390 measurements; contours: 1, 3, 6, 10 and ≥20% per 1% area) in mylonite zones of the Adra Nappe. National grid co-ordinates indicated.

towards the north took place under shallow brittle conditions (Cuevas *et al.* 1986). Within the studied area, south of the Sierra Nevada, the imbricate units of the Adra Nappe only contain garnet and staurolite-bearing schists near the base overlain by biotite schists in the upper parts of the nappe (Fig. 1b).

Three generations of deformational structures have been recognized in the Adra Nappe. The D_1- and D_2-structures are mainly preserved in the biotite schists at high structural levels, in which D_3-structures are less penetrative. The distribution of the D_3-structures is clearly heterogeneous, and provides a structural zoning of the Adra Nappe. Far from the basal contacts of each imbricate, D_3-structures correspond to open asymmetric folds, which deform the S_2-schistosity. They only generate a weak crenulation cleavage in the hinge zones of the more pelitic rocks (Fig. 2a). Towards the basal thrusts a progressive decrease is observed in the interlimb angles of F_3-folds grading into an intense foliation developed in basal mylonite zones. These mylonite zones are characterized by an *L–S* fabrics and *S–C* structures (Fig. 2b). In these mylonite zones pre-mylonite structures can still be recognized, preserved within lozenge-shaped bodies of quartzite, which have been boudinaged during mylonitization (Fig. 2c). The L_3-stretching lineation of the mylonites is defined by biotite and quartz aggregates and has a mean orientation of N45°E (Fig. 1c).

The spatial distribution of these structures in the Adra Nappe reflects an increasing intensity of D_3-deformation towards the basal contacts of the thrust sheets, related to ductile thrusting. Several lines of evidence have been used to argue that these ductile thrusts in the Adra Nappe moved from the SW towards the NE (Cuevas 1988): (1) stretching lineation in the basal mylonites trend N45°E; (2) mesoscopic ductile shear zones in the mylonite zones show a NE sense of displacement; (3) the asymmetry of *S–C* structures consistently indicates a shear sense towards the NE (Fig. 2b); and, finally (4) the geometry of mica-fish (Fig. 2d)

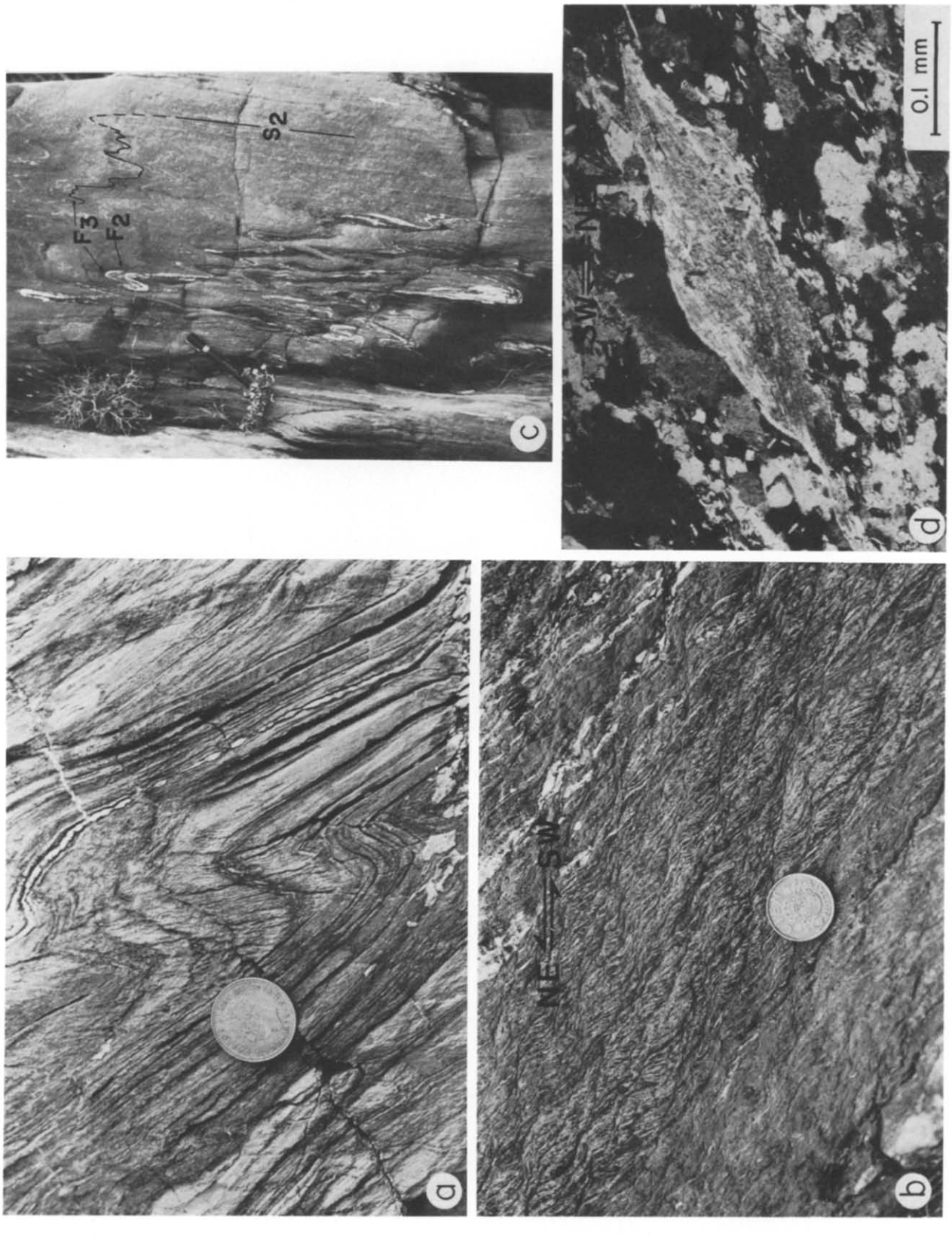

Fig. 2. (a) F_3-folds in biotite-schists from the upper levels of the Adra Nappe. These folds show an axial plane crenulation cleavage (S_3) in the hinge zones and the short limbs. The penetrative S_2-schistosity is parallel to the folded vein of quartz. (b) *S–C* mylonites of type II in garnet–staurolite-bearing schists near the basal contact of a thrust sheet of the Adra Nappe, indicating a top-to-the-NE shear sense. (c) Quartzite layer bounded by mylonitic schists with *S–C* structures. These more competent layers preserve pre-mylonitic structures, such as the S_2-schistosity and even F_2-folds refolded by F_3-folds. (d) *XZ*-thin section of a mylonite showing a mica-fish with an asymmetry consistent with a top-to-the-NE shear sense.

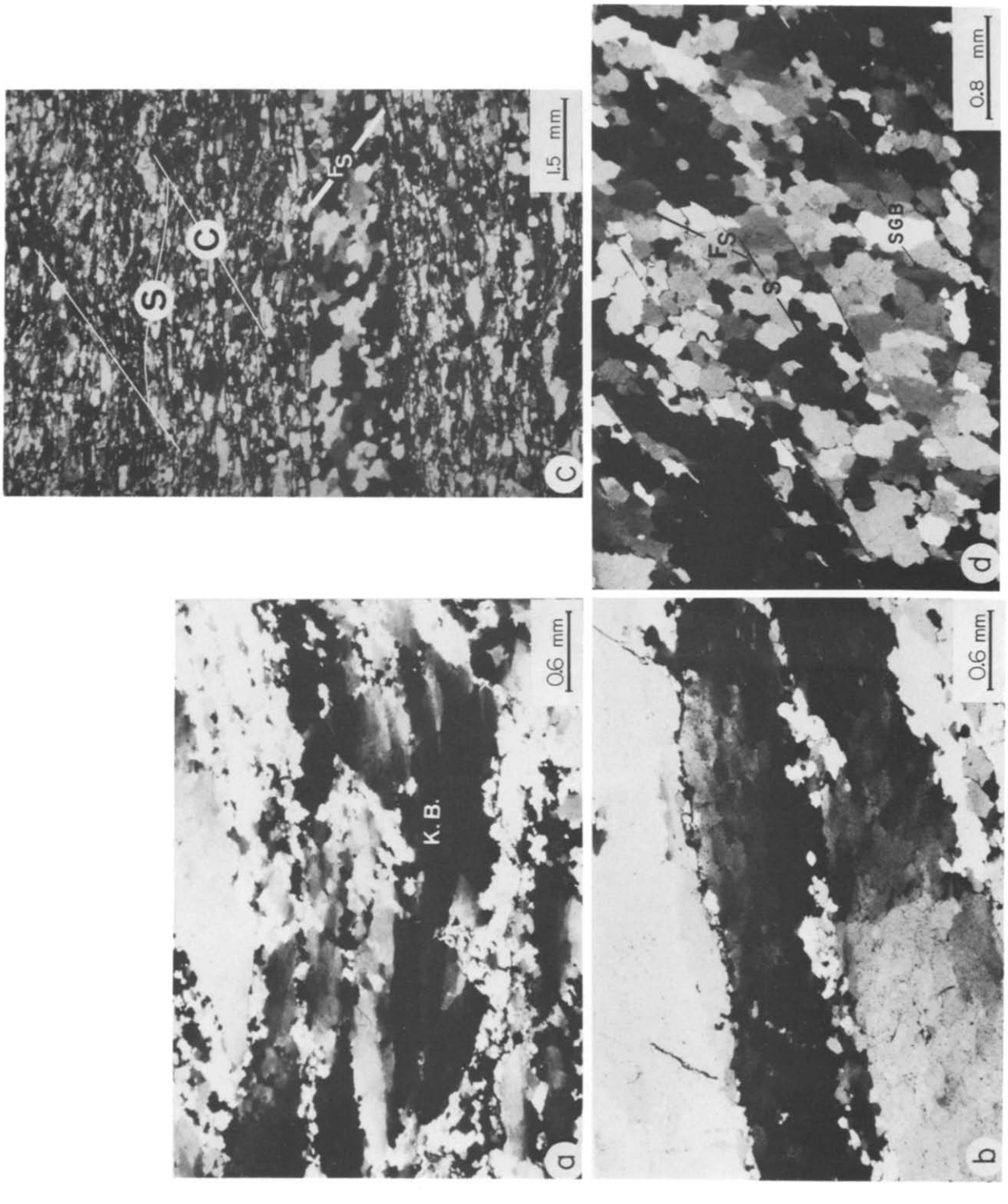

Fig. 3. Microstructures of quartz in *XZ* section. (a) Globular porphyroclast with kink-band subboundaries (K.B.) parallel to the S_2-schistosity and the *c*-axis. (b) Ribbon porphyroclasts bounded by small recrystallized new grains, with *c*-axes subparallel to the S_2-schistosity. (c) Deformed quartz vein enclosed in type II *S–C* mylonites. The shape foliation (f_s) within the vein is oblique to both the shear planes (*C*) and the schistosity (*S*) of the host schists. The asymmetry of *S–C* structures as well as the obliquity of f_s with respect to the schistosity indicates a top-to-the-NE shear sense. (d) Shape foliation (f_s) defined by the arrangement of elongated grains of quartz. f_s is at a large angle to the schistosity, which is marked by the orientation of mica flakes. Numerous boundaries are straight and parallel to sub-grain boundaries (SGB), suggesting that f_s developed during dynamic recrystallization favoured by progressive misorientations at SGBs.

and the asymmetry of pressure-shadows around garnet porphyroclasts indicate a NE sense of movement.

Due to the weak imprint of D_3-structures in the upper levels of the imbricates, the structural framework in those levels corresponds to the S_2-schistosity and the L_2-mineral lineation, whereas down in the basal mylonite zones the structural framework is usually defined by the new S_3-mylonite foliation and the L_3-stretching lineation (Fig. 4).

PETROFABRIC DATA

Quartz fabric development in the Adra Nappe was studied by microstructural analysis of 135 orientated samples and in addition, 25 thin sections from both the mylonite zones and the overlain folded schists were selected to study *c*-axis crystallographic preferred orientation patterns. All microstructural observations and lattice orientation measurements were carried out in XZ sections, that is to say parallel to the stretching lineation and perpendicular to the schistosity. These studies reveal a significant variation of the *c*-axis fabrics, within each imbricate sheet, presumably as a result of the polyphase deformation observed in the Adra Nappe.

Microstructures and c-axis fabrics from the upper part of the Adra Nappe

The quartzites and folded schists in the upper parts of the imbricate units are characterized by an S_2-foliation and by an L_2-lineation, defined by the preferred orientation of mineral aggregates, and by elongated pebbles in deformed metaconglomerates. In thin section, the quartzites show numerous porphyroclasts (0.5–2 mm) derived from old detrital grains in a groundmass formed by small recrystallized grains. The porphyroclasts have been flattened and have an ellipsoidal shape, with their longest axis parallel to S_2. They display deformation bands or undulatory extinction oblique to S_2. The boundaries of the porphyroclasts are affected by recrystallization processes, which contribute to the formation of the groundmass of small new grains. These newly recrystallized grains are equant or slightly elongate depending on whether they occur adjacent to the short or long axis of the porphyroclast, respectively.

The deformed quartz veins present a much more variable microstructure than the quartzites. As in the quartzites, the most common microstructure in the quartz veins is that of quartz porphyroclasts surrounded by a fine-grained matrix of recrystallized new grains. The porphyroclasts have variable sizes (0.4–2 mm) and present rounded as well as ribbon shapes. They are strongly deformed and show optically visible subgrains in some cases and kink-bands in others (Fig. 3a). In these samples many porphyroclasts are globular, in the sense of Bouchez (1977), since they are internally arranged in elongate bands separated by kink-bands parallel to the S_2-foliation (Fig. 3a). The *c*-axes of these porphyroclasts are concentrated near the X-axis of the finite deformation. The ribbon-like porphyroclasts probably represent relics of old globular porphyroclasts, as they usually have their *c*-axes also parallel to the X-axis. This hypothesis is supported by the observation that some kink-bands evolve to grain boundaries (Fig. 3b), probably because they are high strain energy sites from which the recrystallization processes may have started (Avé Lallement & Carter 1970, Post 1977). This process led to a progressive reduction in grain size as well as to a change in the morphology of some globular prophyroclasts from round shapes to ribbon-type porphyroclasts.

Quartz *c*-axis diagrams from the upper parts of the imbricate sheets of the Adra Nappe are shown in Fig. 5. All fabric patterns show a majority of *c*-axes distributed in the periphery of the diagrams close to the XZ-plane, although some diagrams (Ju-42 or Ju-68) show symmetrical patterns, with *c*-axes clustered in four maxima at 45° away from the lineation.

Microstructures and c-axis fabrics from the mylonite zones

Within the mylonite zones of the Adra Nappe the microstructures and the *c*-axis fabrics vary with quartz content in the samples and with their distance from the thrusts. As in the higher structural levels, there are marked microstructural differences between the mylonitized veins of quartz and the quartz microstructure in the surrounding schists (Fig. 3c). In the latter, the size of the quartz grains is invariably smaller than in the mylonitized quartz veins (60–150 μm vs 200–500 μm, respectively). Close to the thrust contacts the mica-bearing quartzites (mica content ~ 10–20%) are characterized by the presence of S–C structures. In these rocks, the quartz grains have elongate grain shapes (X/Z = 2–3)

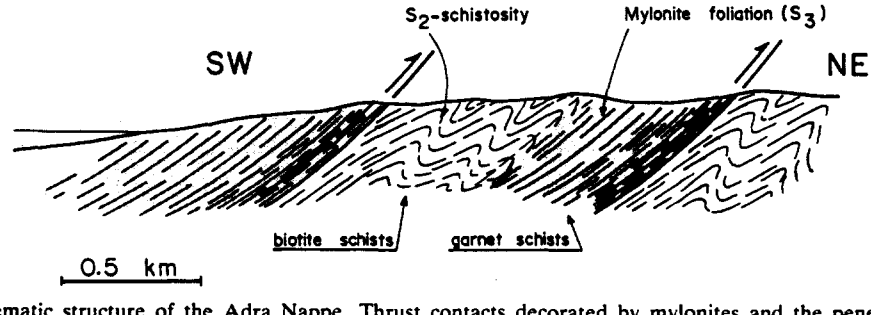

Fig. 4. Schematic structure of the Adra Nappe. Thrust contacts decorated by mylonites and the penetrative planar structures dip southeast. Towards the thrust the S_2-schistosity is gradually obliterated by the mylonite foliation (S_3).

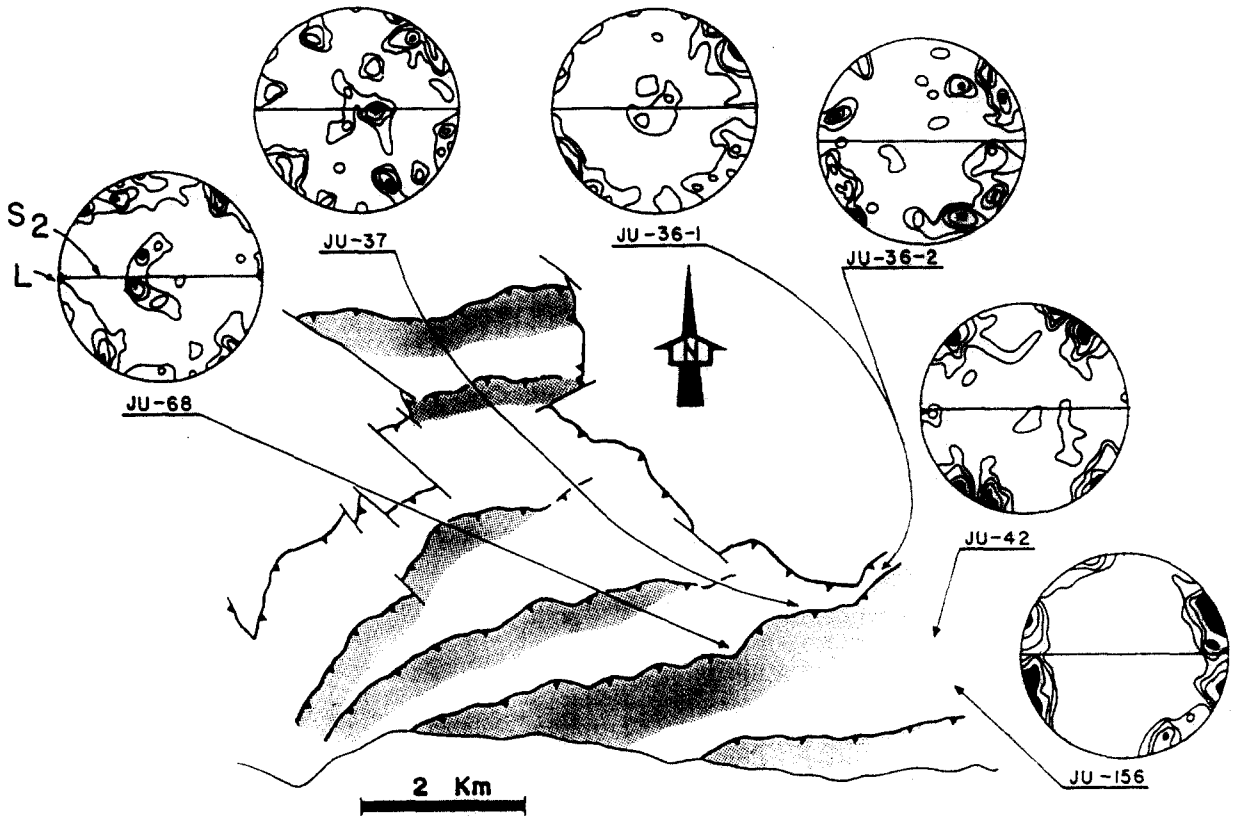

Fig. 5. Quartz *c*-axis diagrams from the upper part of the thrust sheets of the Adra Nappe. Lower-hemisphere, equal-area plots; 150 data per diagram. Contours: 2, 3, 4 and ≥5% (Ju-36-2; Ju-37 and Ju-42); and 2, 3, 5 and ≥7% (Ju-36-1, Ju-68 and Ju-156). The reference frame is defined by S_2-schistosity and L_2-stretching lineation (L).

and are bordered by biotite. The *S*-planes corresponding to the mylonite foliation are defined by the preferred orientation of both the elongate quartz and biotite grains. The grain boundaries at high angles to the foliation have a dentate shape or are bounded by small equant grains which denotes the action of grain boundary migrations in the foliation planes. This also agrees with the presence of small biotite inclusions in the quartz grains. The *C*-planes which obliquely cut the *S*-planes are marked by a considerable decrease in grain size, and by higher aspect ratios and reorientation of the grains. In these tectonites only a few quartz grains are internally arranged in deformation bands. The sub-grain boundaries group together in two families oblique to the *S*-planes (Fig. 6).

In thin section, the quartz veins from the base of the imbricates also show two planar structures, although these structures have a different significance than those of the host schists. The most pronounced one is a shape foliation (f_s) defined by the preferred arrangement of quartz grains with an elongated polygonal shape (Fig. 3d). f_s is oblique to the other planar structure corresponding to the S_3-mylonite foliation, which is determined by the biotite grains contained in the veins. The orientation of f_s forms an angle close to 90° with shear bands visible in the adjacent schists (Fig. 3c). Some quartz grains show sub-grain boundaries which form triple points with the grain boundaries. The sub-grain boundaries are oblique to the mylonite foliation and maintain a uniform sense of asymmetry on a thin section scale (Fig. 6). Usually, the grains with deformation bands are larger than the matrix grains that make up the aggregate and, moreover, often have their long axis parallel to the mylonite foliation. This observation, and the fact that the sub-grain–grain boundaries optically visible in *XZ*-section form an angle of only 12° with f_s, suggest that a major part of the sub-grain boundaries have evolved to grain boundaries by a process of progressive misorientation of the sub-grain. The microstructure is interpreted to result from a recovery process which efficiently contributed to a general grain-size reduction in the tectonites (Poirier & Nicolas 1975, Poirier & Guillopé 1979) and, at the same time, facilitated the destruction of the mylonite foliation in favour of the development of f_s within the quartz veins. The microstructures suggest a cyclic nature of the deformation processes during the mylonitization of the quartz veins, which favoured the development of the mylonite foliation, and recovery processes which tend to destroy it (cf. Law *et al.* 1984, Burg 1986 or Knipe & Law 1987).

Other microstructures such as core and mantle structure (White 1977), or domainal fabrics (García-Celma 1982), are only found in the mylonitized veins farthest away from the thrusts. Some deviation of common microstructures come from the lozenge-shaped enclaves which preserve the pre-mylonite structures in which microstructures similar to those of the quartzite from the upper part of the thrust sheets can be seen.

The quartz *c*-axis fabrics from the mylonite zones can be grouped in several patterns (Fig. 7). A group of

samples shows asymmetric *c*-axis diagrams with respect to the structural frame, with a single-girdle at 50–70° to the mylonitic foliation (Ju-66.V, Ju-75.V, Ju-82, Ju-121). Within such single-girdles *c*-axes show an uneven distribution, although they are mainly concentrated close to the *Z*-axis. Other samples (Ju-69 and Ju-70) are characterized by symmetrical patterns with type I crossed-girdles centred on the *Y*-axis; in this case it can be observed that one of the two girdles is more densely populated than the other. The samples with asymmetric patterns systematically occur in the mylonitized quartz veins nearest to the thrusts, while the symmetrical patterns with two crossed-girdles are representative of the mylonitized schists where the previous quartz veins are enclosed, and also of the mylonitized quartz veins away from the thrust contacts. Finally, some mylonitized quartzites (Ju-73.E) and, specially, the quartzites from the non-mylonitized enclaves (Ju-48.V, Ju-48.E, Ju-39), display diagrams with the *c*-axes distributed preferably in the *XZ* plane, like those coming from the high part of the thrust sheets of the Adra Nappe.

DISCUSSION

The microstructures and *c*-axis fabrics in the mylonite zones provide different kinematic criteria to infer the direction of movement of the Adra Nappe. The quartz microstructures, both grain shape foliations (Fig. 3d) (Burg 1986) and the systematic asymmetry of the sub-grain boundaries (Fig. 6) suggest a top-to-the-NE displacement of the nappe, parallel to the stretching lineation (N45°E) of the mylonites. In addition the sense of the asymmetry of the *c*-axis diagrams (Fig. 7) also indicate this same direction of movement, in agreement with similar interpretations of crystallographic fabrics in other areas (Behrmann & Platt 1982, Bouchez *et al.* 1983, Brunel 1986).

The structures in the Adra Nappe described above suggest a transition of the deformation from a coaxial regime at relatively high levels in the thrust sheets to a non-coaxial regime near the thrusts. The quartz-bearing tectonites also show a systematic variation of the *c*-axis preferred orientation patterns in the nappe. As shown in Fig. 5, at high levels in the thrust sheets symmetric quartz *c*-axis patterns predominate, which points to a coaxial deformation at those levels (Law *et al.* 1986). These symmetrical diagrams are consistent with a deformation at low temperatures, below which only ⟨*a*⟩-slip systems basal planes are activated (Christie *et al.* 1964, Bouchez 1977). On the other hand, they are also consistent with the theoretical predictions of Etchecopar (1974) for the initial stages of a deformation associated with a pure shear flow regime. The concentrations of *c*-axes

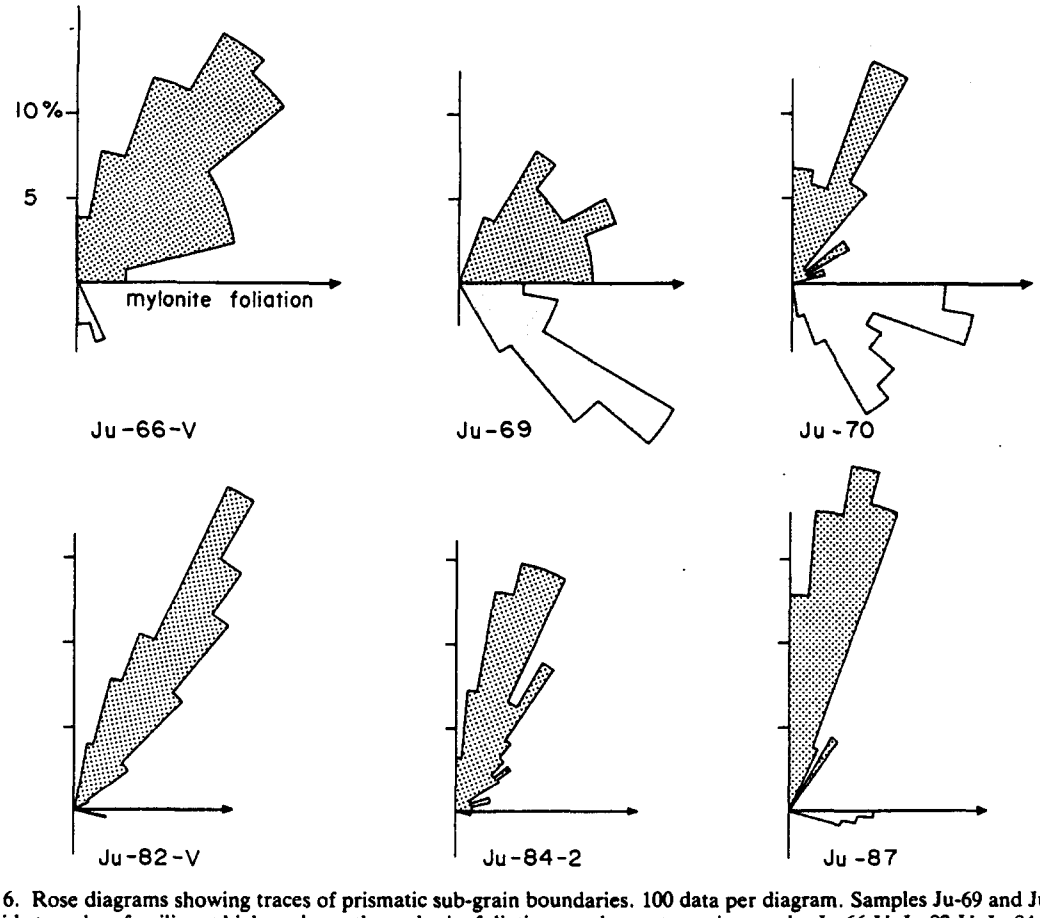

Fig. 6. Rose diagrams showing traces of prismatic sub-grain boundaries. 100 data per diagram. Samples Ju-69 and Ju-70 provide two clear families at high angles to the mylonite foliation; on the contrary, in samples Ju-66-V, Ju-82-V, Ju-84-2 or Ju-87 sub-grain boundaries display one single dominant orientation at a high angle (50–70°) to the mylonite foliation. This change in preferred orientation of the sub-grain boundary traces is associated with the symmetry of *c*-axis patterns (see Fig. 7).

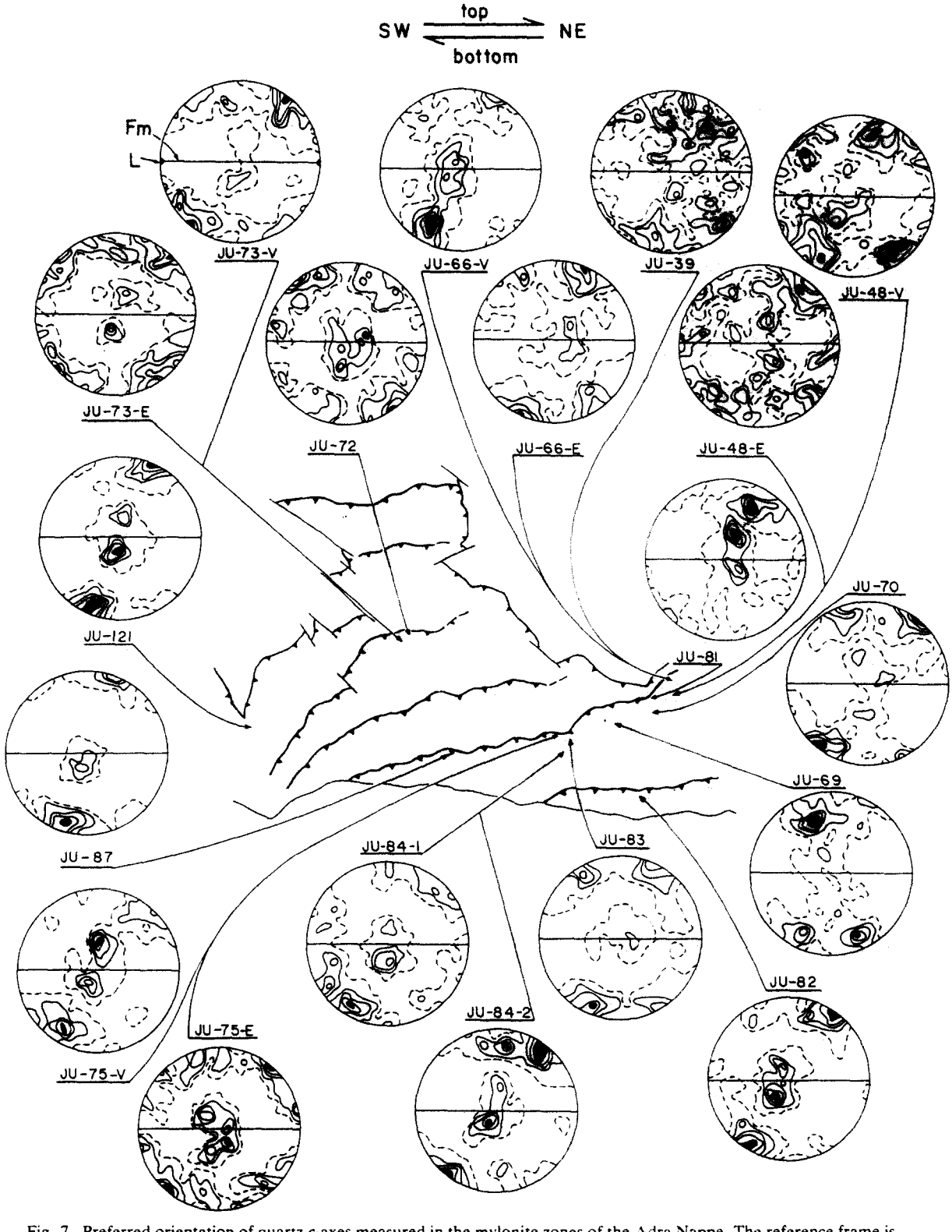

Fig. 7. Preferred orientation of quartz *c*-axes measured in the mylonite zones of the Adra Nappe. The reference frame is defined by mylonite foliation (Fm) and L_3-stretching lineation. Letters V and E refer to mylonitic veins of quartz and biotite quartzites, respectively, in the same thin section. 150 measurements per diagram. Contours: 1, 2, 3, 4 and ≥5% (Ju-39; Ju-48-V; Ju-48-E and Ju-73-V); 1, 2, 3, 5, 7 and ≥9% (Ju-66-V; Ju-66-E; Ju-69; Ju-70; Ju-75-V; Ju-81; Ju-82; Ju-83; Ju-84-2 and Ju-121); 1, 2, 4, 5 and ≥7% (Ju-72; Ju-73-E and Ju-75-E); and 1, 5, 10, 15 and ≥25% (Ju-87). Lower-hemisphere, equal-area plots.

near the *X*-axis could represent grains which have remained in a blocking position during the deformation, as a consequence of an unfavourable initial orientation to become plastically deformed by intracrystalline sliding. As pointed out by Etchecopar (1974) and Bouchez (1977) such grains will develop intracrystalline microstructures like kink-bands, which tend to reduce the size of the grains and to prevent strain hardening processes. The Ju-156 sample, which comes from a quartz vein deformed during the deformation event which originates the S_2-foliation, is an extreme example of a fabric with *c*-axes concentrated around *X*. This

sample, which shows a high proportion of porphyroclasts with kink-bands parallel to the S_2-foliation (Fig. 3a), can be interpreted as a microstructural domain in which the quartz grains developed from former globular porphyroclasts that have partially recrystallized so that the new grains maintain a close orientation relationship with the porphyroclasts (Poirier & Nicolas 1975, Post 1977, White 1977).

Downwards in the nappe towards the mylonite zones along basal thrusts asymmetric single-girdles occur (Fig. 7); this suggests the predominance of a non-coaxial component in the deformation near the thrusts. The observed *c*-axes patterns in the mylonite zones can be explained by intracrystalline ⟨*a*⟩-slip mainly on the (0001) plane and, to a lesser extent, on prismatic planes. These slip systems explain the observed *c*-axis concentrations near the *Z*-axis and the *Y*-axis, respectively (Bouchez 1977, Bouchez & Pêcher 1981). Besides, they attest that the mylonitization occurred at moderate temperatures, which is consistent with the experimental data (Nicolas & Poirier 1976).

A model for fabric transition in the Adra nappe

The quartz fabric of the Adra Nappe reflects a strain variation into a coaxial regime in the interior of the thrust sheets and a non-coaxial regime near the basal thrust of each thrust sheet. As shown by previous fabric studies, the kinematics of flow in mylonites frequently depart from simple shear in numerous ductile shear-zones. This fact has been interpreted in several ways: as the result of the fabric partitioning in a multi-layer (Platt & Behrmann 1986), by a local partitioning of the flow regime for example, near a ramp (Law *et al.* 1984) and also by the sensitivity of the fabric to a last coaxial overprinting (Brunel 1980).

The quartz fabrics in the Adra Nappe could be interpreted as the result of flow partitioning during D_3, in a similar way to those which have been documented by Platt & Behrmann (1986) in the Sierra Alhamilla or by Law *et al.* (1984) in Loch Eriboll; unfortunately, the effects of the D_3-episode at high levels of the thrust sheets, where quartz fabrics are mostly symmetric, are negligible. As an alternative interpretation, we explain the fabric transition across the Adra Nappe in terms of a multi-stage evolution of the deformation which led to symmetric *c*-axis patterns during D_2 and to asymmetric *c*-axis patterns during D_3 (Fig. 8).

As has been indicated previously, the Adra Nappe presents several sets of superimposed structures; however the structural framework corresponds to the S_2-schistosity, except near the thrust where the D_2-structures are usually obliterated by the mylonitization (Fig. 3). These deformational events would also have been recorded by the quartz fabric: the symmetrical patterns of quartz *c*-axis associated to D_2 (Fig. 8a) would only be preserved in domains furthest away from the thrusts, whereas these fabrics would be substituted, to a great extent, by asymmetrical single-girdles during the D_3-deformation, reflecting the simple shear regime associated with the appearance of the thrusts of the Adra Nappe (Fig. 8b).

The structural and petrofabric studies carried out in the Adra Nappe also point to a quartz-fabric partitioning within the mylonite zones: here we find a D_3-flow partitioning between a pure-shear dominated flow at high mylonite levels, where symmetric patterns predominate, and a simple-shear dominated flow near the base, characterized by asymmetric single-girdles. However, even in these mylonite zones there is a fabric-memory of the deformational events preceding the mylonitization. This fabric-memory effect can be recognized by the preservation of some symmetric diagrams of quartz *c*-axes within the mylonite zones of the Adra Nappe.

(i) The samples from lozenge-shaped enclaves of

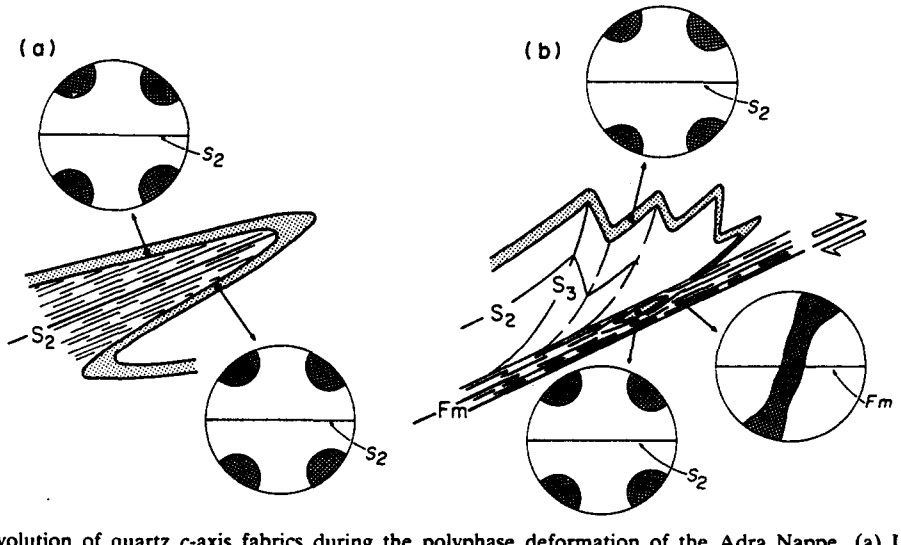

Fig. 8. Evolution of quartz *c*-axis fabrics during the polyphase deformation of the Adra Nappe. (a) Under coaxial conditions where D_2-deformation occurs, the crystallographic preferred orientation of *c*-axes are always symmetrical in relation to the reference frame, defined by S_2. (b) Fabrics related to D_2 are preserved after the subsequent D_3-deformation, except in D_3-mylonite zones where they are replaced by single-girdle fabrics. However, some lozenge-shaped enclaves of boudinaged quartzites within the mylonite zones also preserve pre-mylonitic *c*-axis fabrics.

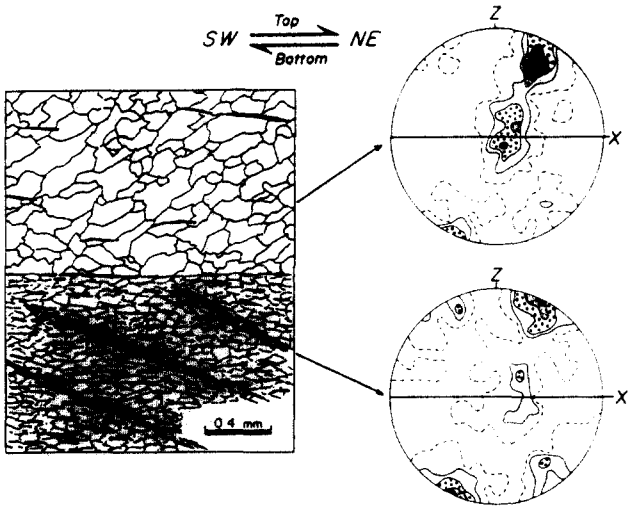

Fig. 9. Microstructural sketch, in *XZ*-section, of a mylonite with a vein of quartz and a biotite-bearing quartzite characterized by a shape foliation (f_s) and *S–C* structures, respectively. Quartz *c*-axis fabrics from these two domains have pronounced differences, as a consequence of the high content of the biotite in the former. All the kinematic criteria indicate a consistent top-to-the-NE motion.

quartzite surrounded by anostomosing mylonite bands provide symmetrical fabric patterns. They show two crossed-girdles in some cases (Ju-69; Fig. 6) or patterns with *c*-axes distributed in the *XZ*-plane in others (Ju-48; Fig. 6); in the latter case there is a tendency for the *c*-axes to be clustered in two maxima at 45° from the stretching lineation. We think these symmetric patterns of *c*-axis can be interpreted as relics of the pre-mylonite fabrics, given that within the enclaves the structures produced during D_2 are preserved. This interpretation is also supported by the similarities between these quartz *c*-axis diagrams models and those obtained in the high part of the thrust sheets.

(ii) Symmetrical patterns of *c*-axes also appear in the mylonite schists with a high proportion (≥20%) of biotite. Usually they display two crossed-girdles, although one of them is often more densely populated than the other (Fig. 9). These *L–S* tectonics have asymmetric pressure shadows around the garnet porphyroclasts and *C–S* structures (Fig. 9) which suggests that the bulk deformation of these rocks involved a flow regime close to simple shear. This interpretation is consistent with the microstructures and *c*-axis fabrics of quartz observable in mm-scale quartz veins parallel to the mylonite foliation (Fig. 9); in fact, these quartz veins show shape foliations and asymmetric single-girdles of quartz *c*-axis, which also point to a non-coaxial deformation. Besides, the sense of shearing provided by the mylonite schists and by the quartz veins contained in them is the same for the different types of kinematic criteria considered (Fig. 9). It can be expected, therefore, that these small areas in which quartz vein and mylonite schists co-exist, have approximately undergone the same flow regime of simple shear. This leads us to attribute the fabric variation in these adjacent rocks with the greater or smaller abundance of quartz in them; the grain sizes suggest, for example, that grain boundary migration mechanisms were more effective in the veins than in the host schists, when the grain size in both is compared (Fig. 3c).

The inclusion of micas at a small inter-particle space not only restricts the growth of grains but also seems to limit the effectiveness of the intracrystalline gliding in the quartz. According to our interpretation not only the intracrystalline gliding of the quartz but also the grain-boundary sliding along biotite–quartz boundaries are active mechanisms during the plastic deformation of the mylonite schists of the Adra Nappe. This would favour part of the quartz grains from the first coaxial fabric remaining in a blocking position to be deformed by intracrystalline gliding during the subsequent deformation (see also Law *et al.* 1986). This hypothesis is supported by the fact that when an *S*-tectonite is affected by a simple shear deformation it channels part of the deformation, reusing the pre-existing anisotropy planes as sliding planes (Brunel 1986). Starting from this, we propose that the two crossed-girdles of the mylonite schists of the Adra Nappe could be interpreted as relics of a coaxial fabric before the mylonitization, which would only have been partially modified by the subsequent simple shear deformation.

CONCLUSIONS

At a regional scale, quartz-fabric data in the Adra Nappe show a strain partitioning into a coaxial regime at the upper part of the thrust sheets and a non-coaxial regime in the mylonite zones located near the basal thrusts. This strain partitioning reflects the action of several deformational events which lead to the development of ductile thrusts in the Adra Nappe.

The variation in the quartz content of mylonite produces significant effects on fabric development. The inclusion of micas at a small interparticle space not only restricts grain growth of the quartz, but also controls the evolution of crystallographic preferred orientations. The dispersion of quartz *c*-axes in biotite-bearing quartzites may indicate deformation resulting from a combination of intracrystalline slip and grain boundary sliding between the quartz and the biotite.

The variation of quartz *c*-axis fabrics across the Adra Nappe can be explained by the ability of quartz fabric to preserve successive events of crystal-plastic deformation in different domains. Such fabric-memory can be recognized within the mylonite zones of the Adra Nappe, which preserve some *c*-axis patterns like those found at higher levels, where the structural framework is defined by pre-mylonitic structures.

Acknowledgements—The financial support is the project PB87-0737-C03-03 of C.I.C.Y.T. (Spain). The paper has benefited from careful reviews by Dr Alvarez, Dr Vissers and Dr Platt. The study was initiated under the management of Dr Bouchez. We are indebted to Denise Whiterlam for her help with the English translation.

REFERENCES

Aldaya, F. 1969. Sobre el sentido de los corrimientos de los mantos

alpujárrides al Sur de la Sierra Nevada (Zona Bética, Provincia de Granada). *Bol. Geol. Min. Espana* **LXXX**, 212–217.

Aldaya, F., García–Dueñas, V. & Navarro-Vilá, F. 1979. Los Mantos Alpujárrides del Tercio Central de las Cordilleras Béticas. Ensayo de correlación tectónica de los Alpujárrides. *Acta Geol. Hisp.* **14**, 154–166.

Avé Lallemant, H. G. & Carter, N. L. 1970. Syntectonic recrystallization of olivine and modes of flow in the upper mantle. *Bull. geol. Soc. Am.* **81**, 2203–2220.

Behrmann, J. H. & Platt, J. P. 1982. Sense of nappe emplacement from quartz *c*-axis fabrics; an example from the Betic Cordilleras (Spain). *Earth Planet. Sci. Lett.* **59**, 208–215.

Bouchez, J. L. 1977. Plastic deformation of quartzites at low temperature in an area of natural strain gradient. *Tectonophysics* **39**, 25–50.

Bouchez, J.-L. & Duval, P. 1982. The fabric of polycristalline ice deformed in simple shear: experiments in torsion, natural deformation and geometrical interpretation. *Text. & Microstruct.* **5**, 171–190.

Bouchez, J.-L. & Pêcher, A. 1981. The Himalayan Main Central thrust pile and its quartz-rich tectonites in Central Nepal. *Tectonophysics* **78**, 23–50.

Bouchez, J.-L., Lister, G. S. & Nicolas, A. 1983. Fabric asymmetry and shear sense in movement zones. *Geol. Rdsch.* **72**, 401–419.

Brunel, M. 1980. Quartz fabrics in shear-zone mylonites: evidence for a major imprint due to late strain increments. *Tectonophysics* **64**, T33–T44.

Brunel, M. 1986. Ductile thrusting in the Himalayas: shear sense criteria and stretching lineations. *Tectonics* **5**, 247–265.

Burg, J.-P. 1986. Quartz shape fabric variations and *c*-axis fabrics in a ribbon-mylonite: arguments for an oscillating foliation. *J. Struct. Geol.* **8**, 123–131.

Burg, J.-P. & Laurent, Ph. 1978. Strain analysis of a shear zone in a granodiorite. *Tectonophysics* **47**, 15–42.

Burg, J.-P., Wilson, C. J. L. & Mitchell, J. C. 1986. Dynamic recrystallization and fabric development during the simple shear deformation of ice. *J. Struct. Geol.* **8**, 857–870.

Carreras, J., Estrada, A. & White, S. 1977. The effects of folding on the *c*-axis fabrics of a quartz mylonite. *Tectonophysics* **39**, 3–24.

Christie, J. M., Griggs, D. T. & Carter, N. L. 1964. Experimental evidence of basal slip in quartz. *J. Geol.* **72**, 734–756.

Cuevas, J. 1988. Microtectónica y metamorfismo de los Mantos Alpujárrides del tercio central de las Cordilleras Béticas (entre Motril y Adra). Unpublished thesis, University of Pais Vasco.

Cuevas, J., Aldaya, F., Navarro-Vilá, F. & Tubía, J. M. 1986. Caractérisation de deux étapes de charriage principales dans les nappes Alpujarrides centrales (Cordillères Bétiques, Espagne). *C. r. Acad. Sci., Paris* **302**, 1177–1180.

Egeler, C. G. & Simon, O. J. 1969. Sur la tectonique de la zone bétique. *Verh. Karin. Neder. Akad. Wetens. Natuur* **XXV**.

Etchecopar, A. 1974. Simulation par ordinateur de la déformation progressive d'un agregat polycristallin. Unpublished thesis, University of Nantes.

Etchecopar, A. 1977. A plane kinematic model of progressive deformation in a polycrystalline aggregate. *Tectonophysics* **39**, 121–139.

García-Celma, A. 1982. Domainal and fabric heterogeneities in the Cap the Creus quartz mylonites. *J. Struct. Geol.* **4**, 443–456.

Julivert, M., Fontboté, J. M., Ribeiro, A. & Conde, L. 1973. Mapa tectónico de la península Ibérica y Baleares (1:1,000,000 scale). *Inst. Geol. Min. España*, Madrid.

Kirby, S. H. 1977. The effects of the α–β phase transformation of the creep properties of hydrolytically-weakened synthetic quartz. *Geophys. Res. Lett.* **4**, 97–100.

Knipe, R. J. & Law, R. D. 1987. The influence of crystallographic orientation and grain boundary migration on microstructural and textural evolution in an *S–C* mylonite. *Tectonophysics* **135**, 155–169.

Law, R. D., Casey, M. & Knipe, R. J. 1986. Kinematic and tectonic significance of microstructures and crystallographic fabrics within quartz mylonites from the Assynt and Eriboll regions of the Moine thrust zone, NW Scotland. *Trans. R. Soc. Edin., Earth Sci.* **77**, 99–125.

Law, R. D., Knipe, R. J. & Dayan, H. 1984. Strain path partitioning within thrust sheets: microstructural and petrofabric evidence from the Moine Thrust Zone at Loch Eriboll, Northwest Scotland. *J. Struct. Geol.* **6**, 477–497.

Lister, G. S. 1981. The effect of the basal-prism mechanisms with on fabric development during plastic deformation of quartzite. *J. Struct. Geol.* **3**, 67–76.

Lister, G. S. & Dornsiepen, U. F. 1982. Fabric transitions in the Saxony granulite terrain. *J. Struct. Geol.* **4**, 81–93.

Nicolas, A. & Poirier, J. P. 1976. *Crystalline Plasticity and Solid State Flow in Metamorphic Rocks*. Wiley-Interscience, London.

Platt, J. P. & Behrmann, J. H. 1986. Structures and fabrics in a crustal scale shear zone, Betic Cordillera, SE Spain. *J. Struct. Geol.* **8**, 15–34.

Poirier, J. P. & Guillopé, M. 1979. Deformation induced recrystallization of minerals. *Bull. Minéral.* **102**, 67–74.

Poirier, J. P. & Nicolas, A. 1975. Deformation-induced recrystallization due to progressive misorientation of subgrains, with special reference to mantle peridotites. *J. Geol.* **83**, 707–720.

Post, R. L. 1977. High temperature creep of Mt. Burnett dunite. *Tectonophysics* **42**, 75–110.

Simpson, C. & Schmid, S. M. 1983. An evaluation of criteria to deduce the sense of movement in sheared rocks. *Bull. geol. Soc. Am.* **94**, 1281–1288.

Tullis, J. A., Christie, J. M. & Griggs, D. T. 1973. Microstructures and preferred orientations of experimentally deformed quartzites. *Bull. geol. Soc. Am.* **84**, 297–314.

White, S. 1977. Geological significance of recovery and recrystallization processes in quartz. *Tectonophysics* **39**, 143–170.